Pressure-induced amorphization and decomposition of $Fe[Co(CN)_6]$

J. Catafesta,[1,2] J. Haines,[3] J. E. Zorzi,[4,1] A. S. Pereira,[1,5,2] and C. A. Perottoni[4,1,*]

[1]*Instituto de Física, Universidade Federal do Rio Grande do Sul, 91501-970 Porto Alegre, Rio Grande do Sul, Brazil*

[2]*PGCIMAT, Universidade Federal do Rio Grande do Sul, 91501-970 Porto Alegre, Rio Grande do Sul, Brazil*

[3]*Institut Charles Gerhardt Montpellier, UMR 5253 CNRS-UM2-ENSCM-UM1, Equipe PMOF, Universit Montpellier II Sciences et Techniques du Languedoc, Place E. Bataillon, cc 003, 34095 Montpellier cedex 5, France*

[4]*Universidade de Caxias do Sul, 95070-560 Caxias do Sul, Rio Grande do Sul, Brazil*

[5]*Universidade Federal do Rio Grande do Sul, Escola de Engenharia, 91501-970 Porto Alegre, Rio Grande do Sul, Brazil*

(Received 4 December 2007; published 12 February 2008)

The high-pressure behavior of the Prussian Blue analogue $Fe[Co(CN)_6]$ has been explored by energy- and angle-dispersive x-ray diffraction, Fourier transform infrared, and Raman spectroscopy. This cyanide-bridged framework material becomes x-ray amorphous above 10 GPa and the high-pressure form is retained upon pressure release. Samples recovered from around 17 GPa exhibit a dark, metallic luster and their Raman spectra are characteristic of amorphous CN_x films. These observations constitute strong evidence that $Fe[Co(CN)_6]$ decomposes at high pressures.

DOI: 10.1103/PhysRevB.77.064104 PACS number(s): 91.60.Gf, 82.30.Lp, 61.43.Er

I. INTRODUCTION

Pressure-induced amorphization (PIA) of negative thermal expansion (NTE) materials has attracted some attention over the past ten years since the first report on PIA of zirconium tungstate.[1] NTE in open framework structures has been explained in terms of low-energy modes whose increase in amplitude leads to contraction on heating.[2,3] However, the precise eigenvalues and eigenvectors of the low-energy modes relevant to the NTE in zirconium tungstate constitute the subject of a still unsettled controversy in the literature.[4–12]

The mechanism originally proposed for the PIA of zirconium tungstate also relates this phenomenon to these low-energy modes. The amorphization of zirconium tungstate should result from the softening of an entire branch of low-energy modes, which freezes the framework structure into a disordered state.[1,13,14] Other mechanisms proposed to explain PIA of ZrW_2O_8 include a hindered decomposition into ZrO_2 and WO_3, and a kinetically impeded transition to a high-pressure, high-temperature crystalline phase.[15,16]

Many compounds that exhibit NTE also amorphize under high pressure (see, for instance, Refs. 17 and 18 and references therein). Recently, anomalous thermal expansion has been observed in several metal-cyanide compounds. In fact, near zero thermal expansion has been reported for the Prussian Blue analogue compound $Fe[Co(CN)_6]$, and isotropic NTE has been found for zinc cyanide, $Zn(CN)_2$.[19,20] The coefficient of thermal expansion for $Zn(CN)_2$ is extremely negative (about twice as that for α-ZrW_2O_8) and becomes even more negative upon pressure increase to 0.5 GPa.[20–22] Furthermore, a recent high-pressure study on $Zn(CN)_2$ has found some evidences of a possible pressure-induced amorphization.[23]

The crystal structure of $Fe[Co(CN)_6]$ (see Fig. 1) resembles that of perovskites, where the metal centered octahedra are not corner shared but, instead, are joined by C-N bridges. This allows these cyanide-bridged framework structures to support a very large number of low-energy modes.[24–26] It is noteworthy to say that, contrarily to ZrW_2O_8 and related compounds, $Fe[Co(CN)_6]$ does not exhibit terminal atoms that could contribute to retain a possible high-pressure amorphous phase back to ambient pressure.[27] From these considerations, it seems worthwhile to verify to what extent the trend between NTE and PIA also applies to nonoxide structures such as these cyanide-bridged framework materials.

In this paper, we report on the pressure-induced amorphization of the near zero thermal expansion material

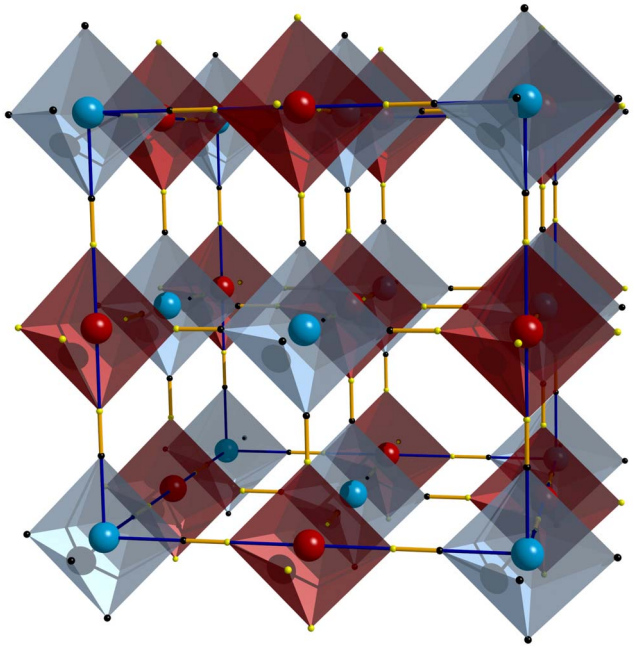

FIG. 1. (Color online) Schematic representation of $Fe[Co(CN)_6]$ crystal structure at ambient pressure (Ref. 19). The light blue and dark red octahedra represent $Co(CN)_6$ and $Fe(NC)_6$ polyhedra, respectively. Carbon and nitrogen atoms are represented by black and yellow spheres, respectively.

$Fe[Co(CN)_6]$. PIA of this compound is supported both by x-ray diffraction and Fourier transform infrared (FTIR) spectroscopy experiments carried out *in situ* at room temperature and high pressure. The samples recovered from high pressure were also analyzed by Raman spectroscopy, which provided conclusive evidences of pressure-induced decomposition. After a brief description of the experimental setup, this paper will proceed with a discussion of the results and an analysis of the possible mechanism behind PIA of $Fe[Co(CN)_6]$.

II. EXPERIMENT

The sample of $Fe[Co(CN)_6]$ used in this work was prepared by precipitation from aqueous solutions of $FeCl_3$ and $K_3[Co(CN)_6]$, as described in Ref. 19. Phase purity was checked by x-ray powder diffraction using a Siemens D500 diffractometer and Cu $K\alpha$ radiation. Energy-dispersive x-ray diffraction (EDXRD) experiments at high pressures were carried out with a Piermarini-Block diamond anvil cell (DAC).[28] The powder sample of $Fe[Co(CN)_6]$ was placed in a 250 μm diameter hole drilled in a Waspaloy gasket preindented to 80 μm, along with a small ruby as pressure gauge and a mixture of methanol-ethanol-water (16:3:1) as pressure-transmitting medium.[29] EDXRD measurements were performed with an intrinsic germanium detector, fixed at $2\theta=10.16°$ ($Ed=70.0$ keV Å), using radiation from a tungsten x-ray tube operating at 45 kV and 20 mA. The radiation was collimated to a beam of 160 μm diameter before reaching the sample in the DAC. Acquisition time was typically 24 h for each spectrum. The energy scale was calibrated against an ^{241}Am source after each spectrum acquisition. Peak positions in the EDXRD spectra were determined by fitting Gaussian profiles to the peaks using the computer program XRDA.[30]

Angle-dispersive x-ray diffraction (ADXRD) was performed in a transmission geometry using the Zr filtered radiation of a Mo microfocus tube. The x-ray beam was collimated to about 100 μm by capillary optics, and the diffraction pattern was recorded on an imaging plate placed at 136.88 mm from the sample for the measurement at atmospheric pressure, and at 143.69 mm for the high-pressure measurements. Exposure times were typically 30–50 h, but longer exposures were made at some pressures to improve the signal-to-noise ratio. The 2θ dependence of the x-ray diffracted intensity was obtained by integration of the diffraction pattern image. The $Fe[Co(CN)_6]$ powder was mixed with NaCl, used as a pressure marker. The sample was loaded into a silica capillary tube for the measurement at atmospheric pressure. The *in situ* ADXRD study under pressure was performed in a lever-arm-type diamond anvil cell. The powder was loaded, without a pressure-transmitting medium, in a 180 μm hole drilled in a tungsten gasket preindented to a 100 μm thickness. The pressure was determined from the equation of state of NaCl.[31]

In situ high-pressure infrared transmission spectra of an $Fe[Co(CN)_6]$ sample dispersed in KBr were obtained with a DAC and a Bomem FTIR model MB100, equipped with a DTGS detector and KBr beam splitter, in the spectral range from 350 to 4000 cm^{-1}. To improve the signal-to-noise ratio, each spectrum comprised 512 scans at 4 cm^{-1} resolution. Pressure was determined with the ruby technique.[29] Raman spectra of the samples processed at high pressure were obtained using a Horiba LABRAM 1B spectrometer and a home-built Raman microprobe consisting of an Olympus BH-2 microscope adapted with a holographic beam splitter and a supernotch filter, a Jobin-Yvon HR320 monochromator, and a EG&G Princeton Applied Research charge coupled device detector. In both cases, a He-Ne laser (632.8 nm) was used as excitation source.

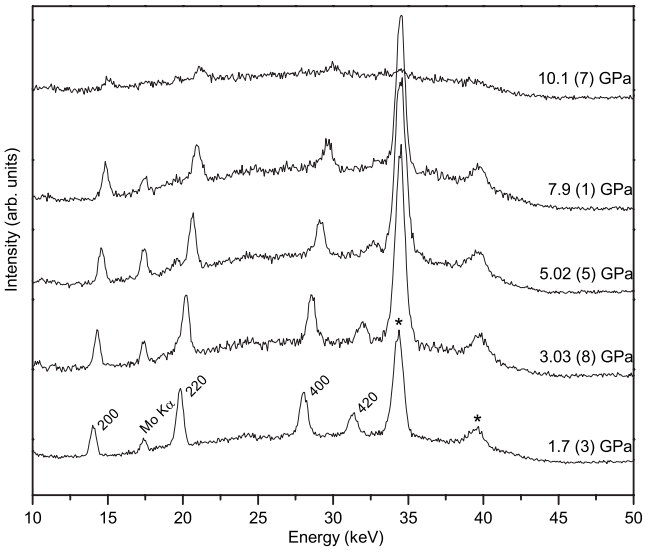

FIG. 2. High-pressure energy-dispersive x-ray spectra of $Fe[Co(CN)_6]$. The Miller indices of Bragg peaks are labeled in the spectrum taken at 1.7 GPa. The Mo $K\alpha$ peak seen in some spectra is a fluorescence peak due to a slit. The asterisks mark diffraction peaks from the gasket.

III. RESULTS AND DISCUSSION

The x-ray diffraction powder pattern of $Fe[Co(CN)_6]$ as synthesized showed no evidence of any contaminant phase and its analysis yielded a lattice parameter [$a_0=10.182(2)$ Å]. The slight difference with respect to the lattice parameters given in the literature may be well accounted for by a small difference in water content.[19] In fact, owing to Vegard's rule and taking into account the results quoted by Margadonna *et al.* for the lattice parameter of $Fe[Co(CN)_6]$ for two different water contents, the actual composition of the sample used in this work can be estimated as $Fe[Co(CN)_6]\cdot 0.2H_2O$.[19]

The first evidence of PIA of $Fe[Co(CN)_6]$ came from the results of EDXRD measurements, as shown in Fig. 2. The intensities of the $Fe[Co(CN)_6]$ Bragg peaks exhibited a noticeable reduction between 7.9 and 10.1 GPa, the maximum pressure reached in this experiment. However, $Fe[Co(CN)_6]$ does not fully amorphize in this pressure range as several Bragg peaks are still clearly visible in the spectrum taken at 10.1 GPa. These peaks are also present in the EDXRD spectrum taken after pressure release, in spite of the fact that the

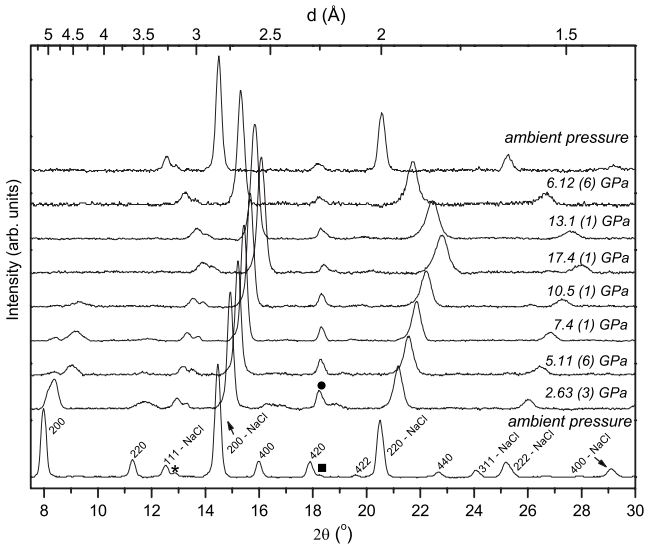

FIG. 3. Angle-dispersive x-ray powder patterns of $Fe[Co(CN)_6]$ (after background removal) from ambient pressure up to 17.4 GPa and back to ambient pressure. The first powder pattern at the bottom shows the Miller indices of $Fe[Co(CN)_6]$ and NaCl Bragg peaks, along with the NaCl 200 and 220 Bragg peaks (marked with * and ■, respectively) associated with the partially filtered $K\beta$ radiation from the Mo x-ray tube. The solid circle (●) on the pattern at 2.63 GPa indicates the position of the most intense peak from the tungsten gasket.

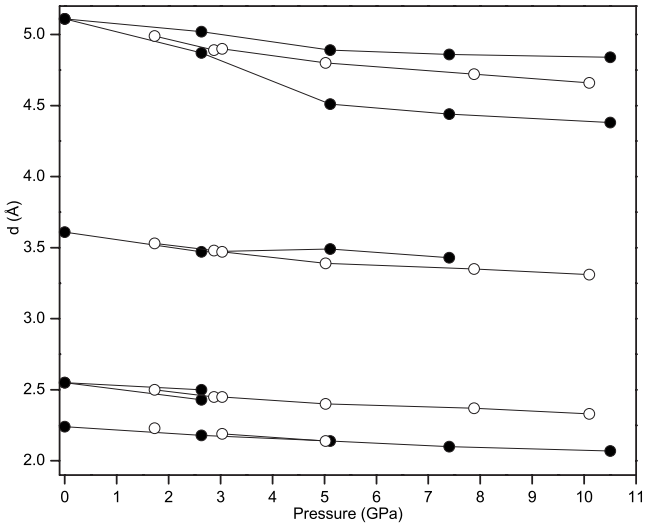

FIG. 4. Pressure dependence of some interplanar distances in $Fe[Co(CN)_6]$. Solid (open) circles refer to ADXRD (EDXRD) results. The lines are just a guide for the eye.

intensities are greatly reduced in comparison to the spectrum taken with the pristine sample. The EDXRD results, thus, provide evidence that at least some part of the $Fe[Co(CN)_6]$ sample undergoes an irreversible loss of crystallinity at high pressures.

A series of angle-dispersive x-ray diffraction measurements were also carried out with $Fe[Co(CN)_6]$. Figure 3 shows the results from this series of measurements up to 17.4 GPa and back to ambient pressure. As for the EDXRD run, some $Fe[Co(CN)_6]$ Bragg peaks remain discernible even at pressures as high as 10.5 GPa. However, the only Bragg peaks which remain visible in the powder pattern at the maximum pressure of this series are those due to NaCl (used as a pressure marker) and the tungsten gasket, showing that the sample has become x-ray amorphous. Besides the severe decrease in peak intensity upon pressure increase, the ADXRD patterns taken at 2.63 GPa and above show a distinct splitting of 200 and 400 peaks. Figure 4 shows the trend between peak positions and pressure from both EDXRD and ADXRD series. The splitting of some Bragg peaks suggests that $Fe[Co(CN)_6]$ may undergo a pressure-induced cubic-to-tetragonal (or even lower symmetry) phase transition before PIA. However, the reduction of peak intensities at high pressures precluded any attempt to assess this possible polymorphic transition and this was not pursued further.

It is worth mentioning that the lack of any sign of the splitting of the 200 and 400 Bragg peaks in the EDXRD results cannot be ascribed only to the intrinsically low resolution of this technique. The marked difference between EDXRD and ADXRD experiments (which refers to the splitting of the 200 and 400 peaks) is probably due to the lack of pressure-transmitting medium in the latter. Indeed, the resulting deviatoric stress field on the sample used in the ADXRD experiment could trigger a structural phase transition toward a lower symmetry phase not observed under more hydrostatic conditions. The interplanar distances for the 200 and 400 peaks determined from the EDXRD spectra are in between the splitted peaks observed in the ADXRD measurements, as expected for a lowering symmetry transition induced by the stress field in the ADXRD experiments. Also, besides the splitting of the 200 and 400 Bragg peaks seen in the ADXRD results, the lack of pressure-transmitting medium may also be influencing the reduction of the intensity of the diffraction peaks at high pressures. In fact, the only Bragg peaks reasonably intense in the ADXRD pattern (obtained without pressure-transmitting medium) at 7.4 GPa are those originated from the 200 peak. On the other hand, all Bragg peaks from $Fe[Co(CN)_6]$ remain clearly visible in the EDXRD spectra obtained at 7.9 GPa. These observations suggest that the state of deviatoric stress over the sample may have a strong influence on the pressure behavior of $Fe[Co(CN)_6]$.

PIA of $Fe[Co(CN)_6]$ was also investigated by *in situ* high-pressure FTIR measurements. Figure 5 shows some representative FTIR spectra of $Fe[Co(CN)_6]$ up to 14.9 GPa and back to 0.15 GPa. The $Fe[Co(CN)_6]$ FTIR spectrum at ambient pressure exhibits bands centered at 478, 592, 802, 933, 1417, 1606, 2180, 2456, 3260, and 3657 cm^{-1}. According to previous studies, the water molecules should partially occupy an interstitial site in the metal-cyanide structure, with the oxygen at the 32*f* position.[19] Indeed, the broad band around 3260 cm^{-1} confirms the presence of some water, and the well defined peak at 3657 cm^{-1} gives further evidence that at least some part of the interstitial water should occupy a well defined site in the crystalline structure. The characteristic bands of the $Fe[Co(CN)_6]$ FTIR spectrum become less distinct as pressure increases, thus giving additional evidence, on a different length scale, that this compound actu-

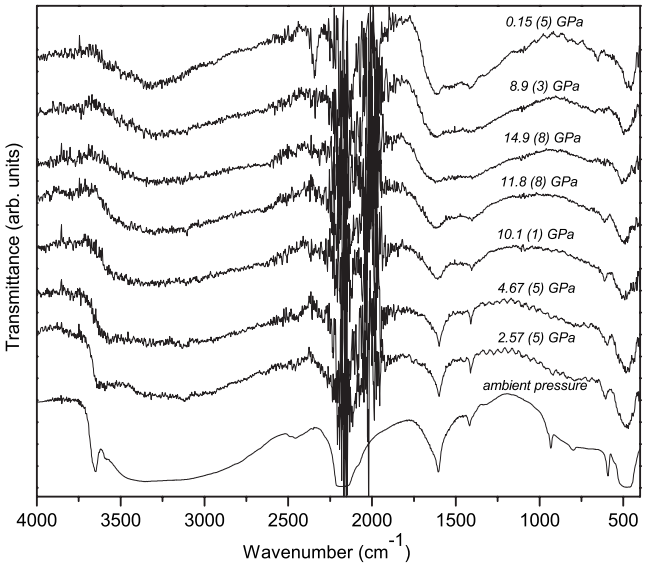

FIG. 5. Some representative FTIR spectra of $Fe[Co(CN)_6]$ up to 14.9 GPa and upon pressure release.

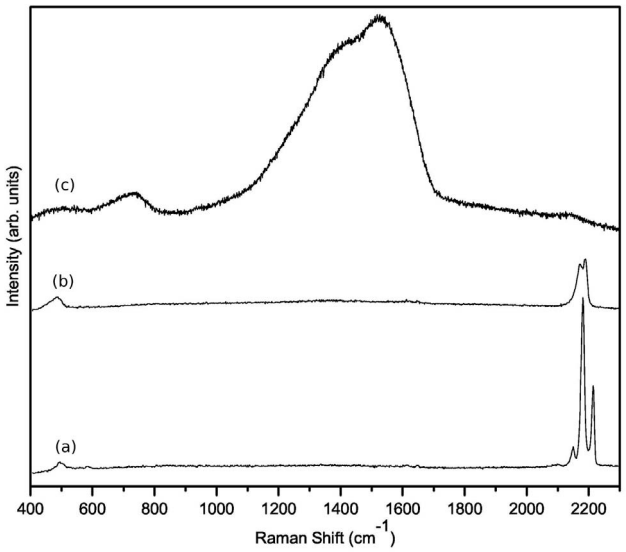

FIG. 6. Raman spectra at ambient pressure of (a) pristine $Fe[Co(CN)_6]$ and of samples previously subjected to (b) 10.1 GPa and (c) 17.4 GPa (this one measured with the Horiba spectrometer).

ally amorphizes above 10 GPa. Furthermore, the FTIR results confirm that the high-pressure form is retained upon pressure release.

Direct visual observation reveals that $Fe[Co(CN)_6]$, originally pale yellow, becomes dark and acquires a metallic luster at pressures above 10 GPa. This dark, metallic aspect remains unaltered in the samples recovered at ambient pressure. The darkening of the sample occurs simultaneously to the marked reduction of the Bragg peaks' intensities, which signals PIA of $Fe[Co(CN)_6]$. Accordingly, both PIA and the darkening effect may have a common origin. Raman spectroscopy provided the clue to unravel this question.

Figure 6 shows the Raman spectra at ambient pressure of pristine $Fe[Co(CN)_6]$ and also of the samples previously subjected to 10.1 and 17.4 GPa (the samples retrieved after the EDXRD and the ADXRD experiments, respectively). The Raman spectrum of pristine $Fe[Co(CN)_6]$ exhibits some small features at 496 and 586 cm^{-1}, along with the characteristic C≡N peaks at 2148, 2181, and 2213 cm^{-1}. The Raman spectrum of the sample previously subjected to 10.1 GPa still exhibits some resemblance to the spectrum of the pristine sample. In fact, this spectrum exhibits broad peaks near 483, 2171, and 2189 cm^{-1}, these latter forming a doublet reminiscent of the former C≡N peaks. On the other hand, the Raman spectrum taken from the sample previously subjected to 17.4 GPa is qualitatively different, with broad peaks centered at 501, 718, 1385, 1551, and 2144 cm^{-1}. The very intense C≡N peaks characteristic of $Fe[Co(CN)_6]$ are now barely visible in the Raman spectrum. The Raman spectrum of the sample recovered from 17.4 GPa closely resembles that of amorphous CN_x films.[32,33] This observation strongly suggests that PIA of $Fe[Co(CN)_6]$ is accompanied by decomposition into an amorphous carbon nitride phase and, possibly, iron/cobalt nanoparticles, which confers the metallic aspect of the samples recovered from high pressures. The pressure-induced decomposition scenario is also supported by the observation of a band centered at 2350 cm^{-1} in the FTIR spectrum at the top of Fig. 5. This band can be assigned to nitrile oxide (—C≡N→O), possibly formed by the interaction of amorphous CN_x with water.[34] The Raman spectrum taken from the sample recovered from 10.1 GPa indicate that $Fe[Co(CN)_6]$ becomes, at least partially, irreversibly disordered even before pressure-induced decomposition takes place, and thus, suggests that this compound may undergo PIA prior to decomposition. This particular subject is currently under study.

IV. CONCLUSION

Pressure-induced amorphization of the Prussian Blue analogue compound $Fe[Co(CN)_6]$ above 10 GPa has been observed on different characteristic length scales by energy- and angle-dispersive x-ray diffraction as well as FTIR and Raman spectroscopy. The Raman spectra of samples of $Fe[Co(CN)_6]$ recovered from high-pressure treatments reveal the formation of amorphous carbon nitride, thus suggesting that PIA of this compound is accompanied by decomposition. The evolution with pressure toward a dark sample, with a metallic luster (possibly resulting from the presence of some iron and cobalt in the metallic state), as well as the observation of an IR absorption band assigned to nitrile oxide in a sample previously subjected to 14.9 GPa are also indicative of decomposition. It remains to be further explored whether amorphization of $Fe[Co(CN)_6]$ occurs as a consequence of or prior to pressure-induced decomposition. The exploration of PIA and decomposition in other cyanide-bridged framework materials which exhibit NTE also deserves further studies.

ACKNOWLEDGMENTS

This work was partially supported by the Brazilian agencies PRONEX/MCT, CNPq, CAPES, and FAPERGS.

*caperott@ucs.br

[1] C. A. Perottoni and J. A. H. da Jornada, Science **280**, 886 (1998).
[2] A. W. Sleight, Annu. Rev. Mater. Sci. **28**, 29 (1998).
[3] A. K. A. Pryde, K. D. Hammonds, M. T. Dove, V. Heine, J. D. Gale, and M. C. Warren, J. Phys.: Condens. Matter **8**, 10973 (1996).
[4] M. G. Tucker, A. L. Goodwin, M. T. Dove, D. A. Keen, S. A. Wells, and J. S. O. Evans, Phys. Rev. Lett. **95**, 255501 (2005).
[5] D. Cao, F. Bridges, G. R. Kowach, and A. P. Ramirez, Phys. Rev. Lett. **89**, 215902 (2002).
[6] D. Cao, F. Bridges, G. R. Kowach, and A. P. Ramirez, Phys. Rev. B **68**, 014303 (2003).
[7] C. A. Figueirêdo and C. A. Perottoni, Phys. Rev. B **75**, 184110 (2007).
[8] T. R. Ravindran, A. K. Arora, and T. A. Mary, Phys. Rev. Lett. **84**, 3879 (2000).
[9] T. R. Ravindran, A. K. Arora, and T. A. Mary, Phys. Rev. B **67**, 064301 (2003).
[10] S. L. Chaplot and R. Mittal, Phys. Rev. Lett. **86**, 4976 (2001).
[11] T. R. Ravindran and A. K. Arora, Phys. Rev. Lett. **86**, 4977 (2001).
[12] J. N. Hancock, C. Turpen, Z. Schlesinger, G. R. Kowach, and A. P. Ramirez, Phys. Rev. Lett. **93**, 225501 (2004).
[13] A. S. Pereira, C. A. Perottoni, and J. A. H. da Jornada, J. Raman Spectrosc. **34**, 578 (2003).
[14] S. M. Sharma and S. K. Sikka, Prog. Mater. Sci. **40**, 1 (1996).
[15] A. Grzechnik, W. A. Crichton, K. Syassen, P. Adler, and M. Mezouar, Chem. Mater. **13**, 4255 (2001).
[16] A. K. Arora, V. S. Sastry, P. Ch. Sahu, and T. A. Mary, J. Phys.: Condens. Matter **16**, 1025 (2004).
[17] T. Varga, A. P. Wilkinson, A. C. Jupe, C. Lind, W. A. Bassett, and C. S. Zha, Phys. Rev. B **72**, 024117 (2005).
[18] S. K. Sikka, J. Phys.: Condens. Matter **16**, S1033 (2004).
[19] S. Margadonna, K. Prassides, and A. N. Fitch, J. Am. Chem. Soc. **126**, 15390 (2004).
[20] D. J. Williams, D. E. Partin, F. J. Lincoln, J. Kouvetakis, and M. O'Keeffe, J. Solid State Chem. **134**, 164 (1997).
[21] T. A. Mary, J. S. O. Evans, T. Vogt, and A. W. Sleight, Science **272**, 90 (1996).
[22] K. W. Chapman and P. J. Chupas, J. Am. Chem. Soc. **129**, 10090 (2007).
[23] T. R. Ravindran, A. K. Arora, S. Chandra, M. C. Valsakumar, and N. V. Chandra Shekar, Phys. Rev. B **76**, 054302 (2007).
[24] K. W. Chapman, M. Hagen, C. J. Kepert, and P. Manuel, Physica B **385-386**, 60 (2006).
[25] A. L. Goodwin and C. J. Kepert, Phys. Rev. B **71**, 140301(R) (2005).
[26] J. W. Zwanziger, Phys. Rev. B **76**, 052102 (2007).
[27] C. A. Figueirêdo, J. Catafesta, J. E. Zorzi, L. Salvador, I. J. R. Baumvol, M. R. Gallas, J. A. H. da Jornada, and C. A. Perottoni, Phys. Rev. B **76**, 184201 (2007).
[28] G. J. Piermarini and S. Block, Rev. Sci. Instrum. **46**, 973 (1975).
[29] G. J. Piermarini, S. Block, J. D. Barnett, and R. A. Forman, J. Appl. Phys. **46**, 2774 (1975).
[30] S. Desgreniers and K. Lagarec, J. Appl. Crystallogr. **27**, 432 (1994).
[31] D. L. Decker, J. Appl. Phys. **42**, 3239 (1971).
[32] A. C. Ferrari, New Diamond Front. Carbon Technol. **14**, 87 (2004).
[33] L. Y. Chen, C. Y. Cheng, and F. C. N. Hong, Diamond Relat. Mater. **11**, 1172 (2002).
[34] D. W. Mayo, F. A. Miller, and R. W. Hannah, *Course Notes on the Interpretation of Infrared and Raman Spectra* (Wiley, Hoboken, 2003), p. 96.